



Contents lists available at ScienceDirect

## DNA Repair

journal homepage: [www.elsevier.com/locate/dnarepair](http://www.elsevier.com/locate/dnarepair)



# Requirement for functional DNA polymerase eta in genome-wide repair of UV-induced DNA damage during S phase

Yannick Auclair<sup>1</sup>, Raphael Rouget<sup>1</sup>, Jonathan M. Belisle, Santiago Costantino, Elliot A. Drobetsky\*

Maisonneuve-Rosemont Hospital, Research Center, Faculty of Medicine, University of Montreal, Montreal, Quebec, Canada H1T 2M4

### ARTICLE INFO

#### Article history:

Received 12 January 2010  
Received in revised form 23 March 2010  
Accepted 29 March 2010  
Available online xxx

#### Keywords:

Nucleotide excision repair  
DNA polymerase eta  
Cyclobutane pyrimidine dimer  
6-4 photoproduct

### ABSTRACT

The autosomal recessive disorder *Xeroderma pigmentosum-variant* (XPV) is characterized (i) at the cellular level by dramatic hypermutability and defective recovery of DNA synthesis following UV exposure, and (ii) clinically by abnormal sunlight sensitivity and remarkable predisposition to skin cancer. These phenotypes are clearly attributable to germline mutations in *POLH*, encoding DNA polymerase eta ( $\text{pol}\eta$ ) normally required for accurate translesion DNA synthesis (TLS) past UV-induced cyclobutane pyrimidine dimers. Here we demonstrate that patient-derived XPV-skin fibroblasts exposed to  $15\text{ J/m}^2$  of UV also exhibit (in addition to abnormal TLS) a significant defect in global-genomic nucleotide excision repair (GG-NER) exclusively during S phase. This cell cycle-specific GG-NER defect can be complemented by ectopic expression of wild-type  $\text{pol}\eta$ , but not of  $\text{pol}\eta$  variants deficient in either nuclear relocalization or PCNA interaction. We highlight a previous study from our laboratory demonstrating that UV-exposed, ATR-deficient Seckel syndrome fibroblasts, like XPV fibroblasts, manifest strong attenuation of GG-NER uniquely in S phase populations. We now present further evidence suggesting that deficient S phase repair can be rescued in both XPV- and Seckel syndrome-cells if the formation of blocked replication forks post-UV is either prevented or substantially reduced, i.e., following, respectively, pharmacological inhibition of DNA synthesis prior to UV irradiation, or exposure to a relatively low UV dose ( $5\text{ J/m}^2$ ). Our findings in cultured cells permit speculation that abrogation of GG-NER during S phase might partially contribute (in a synergistic manner with defective, atypically error-prone TLS) to the extreme state of UV-hypermutability leading to accelerated skin cancer development in XPV patients. Moreover, based on the overall data, we postulate that loss of either functional  $\text{pol}\eta$  or -ATR engenders abnormal persistence of stalled replication forks at UV-adducted sites in DNA which, in turn, can actively and/or passively trigger GG-NER inhibition.

© 2010 Elsevier B.V. All rights reserved.

### 1. Introduction

Within the repertoire of human DNA repair pathways, nucleotide excision repair (NER) alone retains the capacity to remove “bulky DNA adducts” induced by a multitude of environmental mutagens and certain chemotherapeutic drugs. These adducts exhibit great structural diversity, but share in common the ability to distort the DNA helix and to strongly block both DNA replication and transcription. UV-induced cyclobutane pyrimidine

dimers (CPDs) and 6-4 pyrimidine-pyrimidone photoproducts (6-4PPs) have been extensively employed as model bulky DNA adducts to probe the function and regulation of NER [1]. This repair pathway faithfully restores the integrity of UV-damaged DNA through sequential steps of (i) DNA lesion recognition, (ii) unwinding of the DNA duplex around the damaged site, (iii) endonucleolytic incision within a number of bases on either side of the lesion, (iv) excision of the resulting (single-stranded) damaged DNA segment, creating a  $\sim 30$  bp gap and, finally, (v) filling in and sealing of the gap (DNA repair synthesis), using the undamaged complementary strand as template in conjunction with various DNA polymerases/ligases. Two distinct NER subpathways have been characterized which differ only in the manner of lesion recognition: global-genomic NER (GG-NER) and transcription-coupled NER, operating at damaged sites anywhere within the genome and exclusively along the transcribed strand of active genes, respectively [2,3].

Individuals afflicted with “classical” *Xeroderma pigmentosum* (XP) harbour germline mutations in any among seven NER pathway genes, and as a result exhibit defective removal of solar UV-induced DNA photoproducts [4] leading to extreme photosensitivity and

**Abbreviations:** 6-4PP, (6-4) pyrimidine-pyrimidone photoproduct; ATR, ataxia telangiectasia and rad 3-related kinase; CPD, cyclobutane pyrimidine dimer; GG-NER, global-genomic nucleotide excision repair; NER, nucleotide excision repair;  $\text{pol}\eta$ , DNA polymerase eta; TLS, translesion DNA synthesis; XP, *Xeroderma pigmentosum*; XPV, *Xeroderma pigmentosum-variant*.

\* Corresponding author at: Centre de Recherche, Hôpital Maisonneuve-Rosemont, 5415 boul. de l'Assomption, Montréal, QC, Canada H1T 2M4.

Tel.: +1 514 252 3400x4665; fax: +1 514 252 3430.

E-mail address: [elliott.drobetsky@umontreal.ca](mailto:elliott.drobetsky@umontreal.ca) (E.A. Drobetsky).

<sup>1</sup> These authors contributed equally to this work.

remarkably high rates of skin cancer [5]. Patients designated *Xeroderma pigmentosum-variant* (XPV) are clinically indistinguishable from classical XP counterparts; however strong evidence emerged early on that cells derived from the former carry out normal levels of DNA repair synthesis post-UV [6–8]. With only two exceptions to our knowledge [9,10] this was fully supported by subsequent reports [11–13], and in any case to the present day XPV cells are considered to be completely NER proficient. It has also been shown that XPV cells are characterized by (i) moderately increased UV-induced cytotoxicity but dramatically enhanced mutagenicity [14], and (ii) a significant delay in the time required to resume DNA synthesis post-UV [15]. Consistent with the above it was eventually revealed that XPV patients carry germline mutations in *POLH*, encoding DNA polymerase  $\eta$  ( $\text{pol}\eta$ ) [16].  $\text{pol}\eta$  belongs to the Y-family of specialized translesion DNA synthesis (TLS) polymerases (also including  $\text{pol}\mu$ ,  $\text{pol}\kappa$ , and  $\text{REV1}$ ), which collectively are able to replicate past a variety of helix-distorting DNA lesions that otherwise block the progression of normal replicative polymerases [17]. Following UV treatment  $\text{pol}\eta$  specifically becomes activated to bypass highly promutagenic CPDs, which is fortunate given its status as the only Y-family member capable of accomplishing this task with high fidelity [18,19].

As mentioned above, clear evidence has been presented demonstrating that XPV cells are NER proficient. Nonetheless we emphasize that, for technical reasons, a vast majority of previous studies which directly monitored the kinetics of UV DNA photoproduct removal was performed under conditions where replicating (S phase) cells are essentially eliminated from the analysis. In view of this, the primary aim of the current investigation was to compare the NER status of patient-derived XPV-skin fibroblasts vs. wild-type counterparts during each individual phase of the cell cycle. For this purpose we exploited a flow cytometry-based immunoassay, recently developed and validated in our laboratory, which permits quantification of GG-NER kinetics as a function of cell cycle [20]. We report here (i) that primary XPV-skin fibroblasts irradiated with UV exhibit profound deficiency in GG-NER during S phase, whereas repair during either G0/G1 or G2/M remains unaffected (GG-NER occurring in S phase is hereafter denoted S Phase Repair; SPR), and (ii) that this cell cycle-specific repair defect is attributable to loss of functional  $\text{pol}\eta$ . Of note we previously demonstrated that Seckel syndrome fibroblasts irradiated with UV also exhibit a significant reduction in SPR efficiency, specifically due to genetic abrogation of ATR kinase signaling [20]. We further reveal here that normal SPR can be restored in either XPV- or Seckel syndrome-cells by abolishing or substantially reducing the incidence of stalled replication forks at UV-adducted sites in DNA. Our findings may potentially provide some novel insight into the molecular underpinnings of XPV-associated UV-hypermutable leading to skin cancer development. The overall data in XPV- and Seckel syndrome-cells suggest that GG-NER can be actively and/or passively inhibited under conditions of particularly severe UV-induced

replicative stress, possibly resulting in enhanced cellular survival at the cost of greatly increased mutagenesis (see Section 4).

## 2. Materials and methods

### 2.1. Cell culture

Wild-type primary skin fibroblasts (GM01652B) and three patient-derived XPV primary skin fibroblast strains (XP115LO, XP30RO, and XP5MA) were obtained from the Coriell Institute. The SV40-transformed XPV-skin fibroblast strain XP30ROsv, and its isogenic derivative ectopically expressing wild-type  $\text{pol}\eta$  (XP30ROsv- $\text{pol}\eta/\text{cl6}$ ), were kindly provided by Dr. A.R. Lehmann (University of Sussex). Primary LL lung fibroblasts were a gift of Dr. J. Sedivy (Brown University). The hTERT-immortalized Seckel syndrome skin fibroblast strain F02-98 and the closely related wild-type counterpart 1BR were obtained from Dr. P. Jeggo (University of Sussex). All primary strains were cultured in Eagle's MEM supplemented with 15% foetal bovine serum, L-glutamine, and antibiotics (Wisent, Montreal, Canada). SV40-transformed and hTERT-immortalized cells were grown in Dulbecco's MEM supplemented as above.

### 2.2. Construction and ectopic expression of EGFP-tagged $\text{pol}\eta$ variants

Trizol<sup>TM</sup>-extracted total RNA from primary GM01652B skin fibroblasts was employed to synthesize a cDNA encoding full-length wild-type (wt)  $\text{pol}\eta$  by RT-PCR using primer pairs XPV1 (ATGGCTACTGGACAGGATCGAGT) and XPV2 (GGCAGCACTAATGTGTTAATG GCTT). The wt cDNA was then subcloned into the pGemT-Easy vector (Promega), which in turn was used as substrate to amplify the  $\text{pol}\eta$ -wt and  $\text{pol}\eta$ - $\Delta\text{Ct}$  cDNAs via PCR using *pfu* DNA polymerase (Stratagene) and primer pairs containing *XhoI* and *EcoRI* restriction sites (Table 1). These PCR products were cloned, in phase with EGFP at the C-terminal end of  $\text{pol}\eta$ , into the expression vector pEGFP-N1 (Clontech). The EGFP-tagged  $\text{pol}\eta$  mutant, termed here  $\text{pol}\eta$ -PIP1/2, was obtained by site-directed mutagenesis as described [21] using  $\text{pol}\eta$ -wt-pEGFP-N1 in conjunction with appropriate mutagenic primer pairs (Table 1). The DNA sequences of all EGFP- $\text{pol}\eta$  fusion vectors were verified by automated dideoxy sequencing (Core Sequencing Facility, University of Montreal).

XP30ROsv cell populations stably expressing each of the EGFP- $\text{pol}\eta$  fusion vectors were derived by transfection in the presence of Lipofectamine 2000<sup>TM</sup> (Invitrogen), followed by selection using 200  $\mu\text{g}/\text{ml}$  G418 (Wisent, Montreal, Canada). Enrichment for EGFP-expressing cells was then performed by fluorescence-activated cell sorting (FACS Vantage SE DiVa option equipped with a 70  $\mu\text{m}$  nozzle at 25PSI; Becton-Dickinson). Briefly cells were sorted based on EGFP autofluorescence level, cultured for seven days, re-sorted, and then cultured again for an additional week. Prior to experimentation

**Table 1**  
Primer pairs used for cloning  $\text{pol}\eta$ -wt and  $\Delta\text{Ct}$  cDNA in phase into pEGFP-N1 and for site-directed mutagenesis.

cDNA	Primers	Restriction sites	Sequence (5' → 3')
$\text{pol}\eta$ -wt	Forward	<i>XhoI</i>	GGACCGCTCGAGATGGCTACTGGACAGGAT
	Reverse	<i>EcoRI</i>	CTTTTCCTTGAATTCGATGTGTTAATGG
$\text{pol}\eta$ - $\Delta\text{Ct}$	Forward	<i>XhoI</i>	GGACCGCTCGAGATGGCTACTGGACAGGAT
	Reverse	<i>EcoRI</i>	CTTTTCCTTGAATTCGTACCAAGGAGCCACACTT
Mutant	Point mutations	Mutagenic primers	Sequence (5' → 3') <sup>a</sup>
$\text{pol}\eta$ -PIP1/2	F443A; L444A (PIP1 mut)	Forward	TCTACAGACATCACCAGCGCCGCGAGCAGTGACCCAAGTTC
		Reverse	GAACTTGGGCTACTGCTCGCGGCGCTGGTGATGCTCTGTAGA
	F707A; F708A (PIP2 mut)	Forward	CAAACATTGGAATCAGCTGCTAAGCCATTAAACACATTAG
		Reverse	CTAATGTGTTAATGGCTTAGCAGCTGATTCCAATGTTTG

<sup>a</sup> Mutated sites in bold.

(i) EGFP autofluorescence was verified by flow cytometry and (ii) expression of each EGFP-pol $\eta$  fusion protein evaluated by immunoprecipitation and Western blotting using the primary polyclonal and monoclonal-anti-POLH antibodies H-300 and B7, respectively (Santa Cruz).

### 2.3. UV irradiation

Cell monolayers were washed thoroughly with phosphate-buffered saline (PBS) and covered with 2 ml of PBS, followed by exposure to 254-nm UV using a Philips G25T8 germicidal lamp. The UV fluence was 0.2 J/m<sup>2</sup>/s as measured with a DRC100X digital radiometer equipped with DIX254 sensor (Spectroline Corporation).

### 2.4. Protein detection by Western blotting

Pol $\eta$  was detected by immunoprecipitation and Western blotting as described [22,23]. The supernatant was stored at -80 °C and used in conjunction with anti-actin antibody to verify that equal total protein had been employed for the immunoprecipitation (loading 5% of total input).

To evaluate siRNA knockdown of pol $\eta$  in primary LL lung fibroblasts, chromatin-bound protein was detected using a protocol that initially removes soluble polypeptides by extraction in cytoskeleton buffer (CSK; 10 mM Pipes (pH 6.8), 300 mM sucrose, 100 mM NaCl, 3 mM MgCl<sub>2</sub>, 1 mM EGTA, 20 mM vanadyl ribonucleoside complex, 1 mM 4-(2-aminoethyl)benzenesulfonyl fluoride). Specifically, 1 × 10<sup>6</sup> cells were lysed with 0.5% Triton-X-100/CSK for 15 min on ice and centrifuged. The pellets were incubated with 0.5% Triton-X-100/CSK buffer for an additional 15 min, centrifuged, and resuspended in 30  $\mu$ l 1 × Laemmli buffer for Western blotting. Pol $\eta$  was detected using anti-POLH polyclonal antibody (H-300; Santa Cruz, 1:1000 dilution). As loading control, the membrane was stripped and re-hybridized with anti-PCNA antibody (PC-10, Santa Cruz).

### 2.5. Localization of ectopically expressed pol $\eta$ -EGFP fusion proteins in XP30ROsv cells

Cells were grown for 24 h on glass coverslips in 35-mm culture dishes, fixed with 3.7% paraformaldehyde for 20 min at room temperature, followed by thorough washing with PBS. Cells were mounted with ProLong™ Gold antifade reagent containing DAPI counterstain (Molecular Probes–Invitrogen). Stained cells were then photographed and analyzed using an inverted fluorescence Zeiss Axio Observer A1 microscope equipped with QICAM FAST 1394 camera (QImaging, Canada) and Northern Eclipse software (Empix Imaging Canada).

### 2.6. Live cell imaging of pol $\eta$ nuclear foci

XP30ROsv cells (6 × 10<sup>4</sup>) expressing either EGFP-pol $\eta$ -wt or EGFP-pol $\eta$ -PIP1/2 were seeded on 35-mm glass-bottom dishes and cultured for 24 h in Opti-MEM medium (Invitrogen) supplemented with 10% FBS and antibiotics. Live cells were irradiated, or mock-irradiated, with 15 J/m<sup>2</sup> of UV and analyzed using a fluorescence microscope (IX71 Olympus, Japan) with a 100 × 1.45NA oil immersion objective. The images were acquired with a Retiga 2000R CCD (QImaging, Canada). The microscope was equipped with a MAX201 motorized stage (Thorlabs, NJ), and both the stage and camera were controlled by a custom program written in Labview (National Instrument, TX) to acquire 100 (10 × 10) contiguous images covering a 1.18 mm × 0.88 mm region with submicron resolution. The same region was imaged before, and 1.5 h after, UV irradiation.

Nuclear foci were detected and quantified using an automatic custom image analysis program written in MatLab (Mathworks, MA). To perform this quantification, an intensity threshold was first established using the method of Otsu [24]. Foreground pixels were used as masks to specifically select nuclei. A two-dimensional filter using Gaussian kernel was applied to detect only elements of a certain size (approximately 0.5  $\mu$ m) and foci were identified as local maxima. At least 50 cell pairs were analyzed in the case of each EGFP-pol $\eta$ -expressing XP30ROsv strain.

### 2.7. siRNA-mediated depletion of pol $\eta$

Cells (2 × 10<sup>5</sup>) were seeded on 35 mm dishes in complete growth medium without antibiotics. After 24 h, each culture was transfected with siRNAs targeting human pol $\eta$  (sc-36289), or nontargeting control siRNAs (sc-37007) (Santa Cruz), employing Lipofectamine 2000 according to the manufacturer's directions (Invitrogen). Cells were used for experiments at 2 days post-transfection after verifying pol $\eta$  knockdown by Western blotting.

### 2.8. Treatment with DNA synthesis inhibitors

Cells were cultured for 2 h in fresh complete medium containing either 15  $\mu$ g/ml aphidicolin (Sigma) or 10 mM hydroxyurea (Sigma). The medium was then removed, and cells thoroughly washed with PBS followed by UV irradiation in PBS. Fresh complete medium without inhibitor was added for post-UV incubations.

### 2.9. Clonogenic survival

Exponentially growing cultures on 100-mm dishes were irradiated with 0, 7.5, or 15 J/m<sup>2</sup> of UV, and immediately trypsinized for plating of appropriate cell numbers on 100-mm dishes in fresh complete medium. Following 15 days incubation, colonies were stained with 0.5% methylene blue (w/v) in 50% methanol (v/v). Survival is expressed as a percentage relative to mock-irradiated cells.

### 2.10. Determination of GG-NER kinetics as a function of cell cycle

The removal of 6-4PPs in each phase of the cell cycle was monitored over a 6 h period as previously described [20] with the following exception. In the case of XP30ROsv cells stably expressing EGFP-pol $\eta$  fusion proteins, since EGFP autofluorescence interferes with the FITC signal, Alexa-Fluor700-conjugated goat anti-mouse antibody (Molecular Probes–Invitrogen, dilution 1:400) was used as secondary antibody in place of FITC-conjugated rabbit anti-mouse antibody. The acquisition was performed using an LSRII flow-cytometer (Becton-Dickinson) equipped with argon (blue, 488 nm)- and helium–neon (red, 633 nm)-lasers.

For cell cycle-specific evaluation of CPD repair kinetics up to 24 h, to control for cellular proliferation during post-UV incubations, a triple-labeling approach employing BrdU in conjunction with PI and anti-CPD antibody was optimized. Monolayers at 50% confluence were irradiated with either 5 or 15 J/m<sup>2</sup> of UV. For time zero (0 h) cells were pulsed for 30 min with 30  $\mu$ M of BrdU, irradiated, and then immediately harvested. For later time points, to avoid potential artefacts associated with BrdU photolysis, cells were pulsed for 30 min immediately following irradiation, rinsed with PBS, and re-fed with fresh medium for the remaining incubation period. At the various time points, monolayers were washed with PBS, trypsinized, resuspended in 1 ml of PBS, and fixed by addition of 3 ml of ice-cold 100% ethanol. Fixed cells (5 × 10<sup>5</sup>) were pelleted, washed with PBS, and incubated for 20 min at 22 °C with 0.5% Triton-X-100 in 2N HCl followed by centrifugation and resuspension in 0.1 M Na<sub>2</sub>B<sub>4</sub>O<sub>7</sub> pH 9 for 20 min. Cells were washed

with PBS, resuspended in 300  $\mu$ l of RNase solution (100  $\mu$ g/ml in PBS), incubated for 1 h, and washed with 1 ml of PBS-TB (1% BSA/0.25% Tween-20/PBS). Cells were then centrifuged and resuspended in 300  $\mu$ l of PBS-TB containing anti-CPD antibody (Kamiya Biomedical Company; 1:1000 dilution), incubated for 1.5 h at 22 °C, washed twice with PBS-TB, and incubated with FITC-conjugated rabbit anti-mouse secondary antibody (Sigma; 1:200) in 300  $\mu$ l PBS-TB at 22 °C for 1 h in the dark. Cells were rinsed once with PBS-TB and incubated for 15 min with IgG isotype control (Invitrogen; 1:100 dilution). After washing with PBS-TB, cells were incubated with an Alexa-Fluor647-conjugated anti-BrdU antibody (Molecular Probes-Invitrogen; 1:200 dilution) in PBS-TB for 1 h, rinsed with PBS-TB, centrifuged and resuspended in PBS containing 5  $\mu$ g/ml of PI, and finally analyzed using a FAVCS-caliber flow cytometer (Becton-Dickinson, USA). Fluorescence intensity of UV photoproducts was obtained by gating the appropriate phase of the cell cycle on a bivariate dot plot. Quantification of the change in geometric mean fluorescence of the population over time indicates repair.

### 3. Results

#### 3.1. DNA repair status of XPV-skin fibroblasts revisited

The efficiency of 6-4PP removal as a function of cell cycle was initially quantified in four primary skin fibroblast strains: wild-type

GM01652B vs. the XPV strains XP115LO, XP5MA, and XP30RO. The latter three strains are reported to carry severe pol $\eta$  truncations and no detectable full-length protein, which was substantiated by Western blotting (Fig. 1A). Moreover in line with previous observations [25], XPV fibroblast strains displayed moderately decreased long-term clonogenic survival post-UV relative to the wild-type counterpart (Fig. 1B). For DNA repair rate determinations, briefly, replicate cultures were irradiated with 15 J/m<sup>2</sup> of UV and incubated for 0, 1.5, 3, or 6 h. Following harvesting, fixation, and permeabilization, cells were incubated with fluorescently labeled anti-6-4PP antibody and co-stained with propidium iodide (PI). Flow cytometry was then used to analyze the extent of 6-4PP removal for populations gated in each phase of the cell cycle, as graphically depicted for all primary skin fibroblast strains (Fig. 1C). A representative bivariate dot plot (Fig. 1D; upper panel) and histogram overlay (Fig. 1D; lower panel) show raw data for XP115LO. It is well established that 6-4PP repair in human fibroblasts is virtually complete (80–100% removal) by 6–8 h post-UV [26]. In accord with this (and as we previously observed [20]), wild-type GM01652B fibroblasts exhibit >90% repair of 6-4PP during either G0/G1 or G2/M by 6 h following UV treatment, and a very moderate but significant slowdown during S (80% removal) (Fig. 1C). Strikingly, however, each of the XPV strains XP115LO, XP5MA, and XP30RO is shown to be significantly defective in 6-4PP removal during S, while displaying characteristically rapid repair kinetics during other phases.

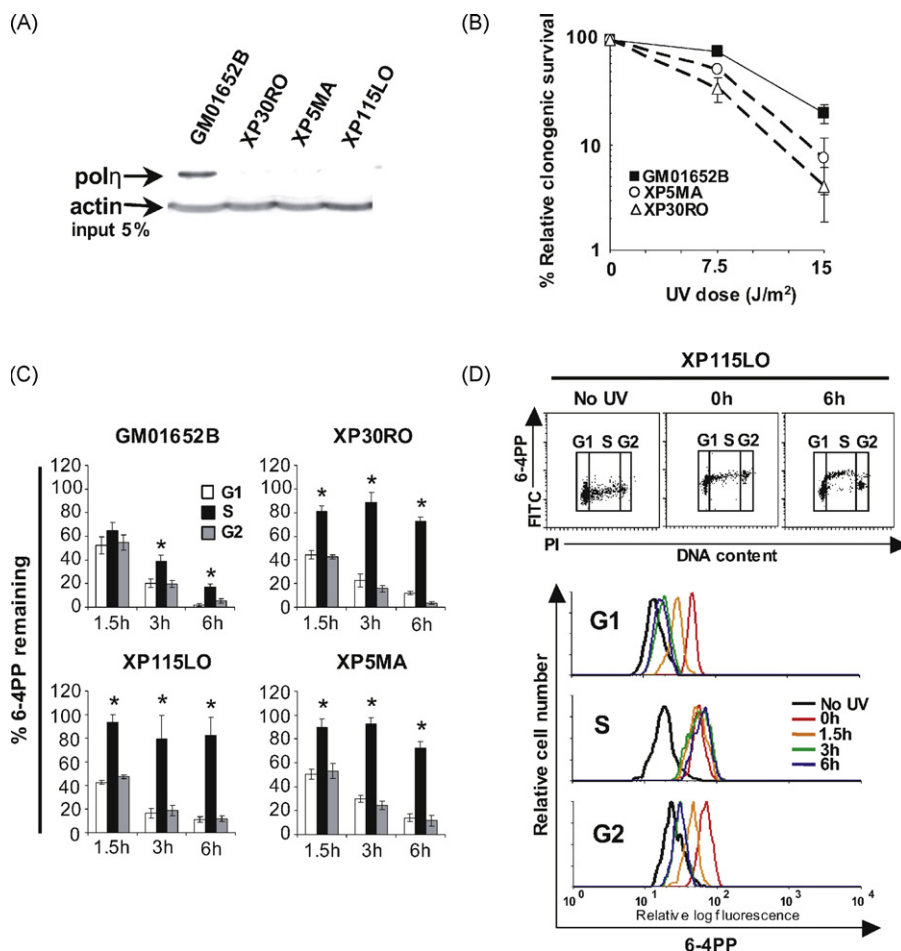


**Fig. 1.** SPR of 6-4PPs is defective in primary XPV-skin fibroblasts. (A) Detection of pol $\eta$  in XPV vs. wild-type primary skin fibroblasts by immunoprecipitation and Western blotting. (B) Relative clonogenic survival in UV-irradiated wild-type-skin vs. XPV-skin fibroblasts. Shown is the mean  $\pm$  SEM from three independent experiments. (C) Graphical depiction of repair in wild-type-skin vs. XPV-skin fibroblasts irradiated with 15 J/m<sup>2</sup> of UV. Shown is the mean  $\pm$  SEM of four independent experiments. \* $p$  < 0.05; two-tailed paired  $t$ -test (S phase relative to G1). (D) Representative results illustrating cell cycle-specific 6-4PP repair in the XPV strain XP115LO. Upper panel; bivariate distribution of 6-4PP (FITC) versus DNA content (PI) at 0 and 6 h post-UV, and in unirradiated cells (no UV); lower panel; histogram overlay showing repair of 6-4PPs in each phase of the cell cycle.

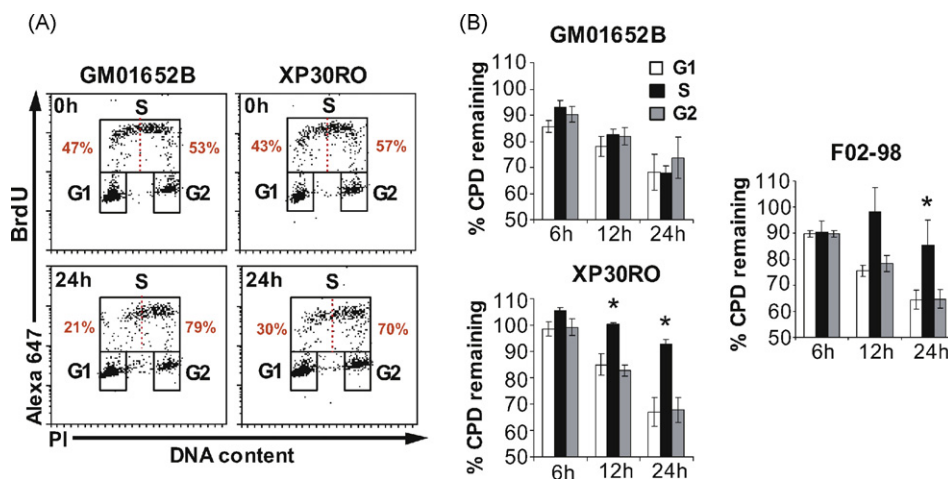


**Fig. 2.** SPR of CPDs is defective in primary XPV-skin fibroblasts. (A) Bivariate distribution of BrdU incorporation (Alexa 647) vs. DNA content (PI) in GM01652B vs. XP30RO at 0 h vs. 24 h post-UV. The red dotted line and numerals indicate the percentage of cells in early- vs. late-S phase. (B) Graphical depiction of cell cycle-specific CPD repair in GM01652B, XP30RO, and F02-98 cells irradiated with  $15\text{ J/m}^2$  of UV. Shown is the mean  $\pm$  SEM of three independent experiments. \* $p < 0.05$ ; two-tailed paired  $t$ -test (S phase relative to G1).

The initial induction level of CPDs post-UV is 3–5 times higher than 6-4PPs; moreover the former adduct is excised with much slower kinetics, i.e., only 30–40% CPD removal by 24 h post-UV, compared with the relatively very rapid 6-4PP repair rate as discussed immediately above. For these and other reasons, CPDs as opposed to 6-4PPs have been considered the preeminent cause of sunlight-induced mutations leading to skin cancer development [27]; thus any defect in CPD repair *per se* could conceivably represent an important factor in XPV pathogenesis. Moreover efficient removal of either CPDs or 6-4PPs can vary according to genetic background, e.g., reduced GG-NER of CPDs but not of 6-4PPs in cells lacking a functional p53 tumour suppressor [28], or in XPE fibroblasts characterized by deficiency in the GG-NER lesion recognition protein DDB2 [29]. Finally we were interested to probe whether defective SPR in XPV cells could persist for as long as 24 h post-UV. The above considerations highlighted the importance of confirming whether SPR of CPDs, in addition to 6-4PPs, is defective in XPV cells.

However quantification of CPDs as a function of cell cycle, relative to the situation for 6-4PPs, poses a distinct technical challenge. Indeed the precision of our cell cycle-specific GG-NER assay depends upon the ability to tightly control for movement of cells between various growth phases during post-UV incubations. It is well established that UV-exposed cultured cells exhibit a transient period of growth arrest and inhibition of DNA synthesis, the length of which depends upon dose as well as cellular capacity to remove replication-blocking UV DNA photoproducts [30,31]. Consistent with this we have observed that all strains used herein exhibit complete arrest of cell cycle progression for at least 6 h post-irradiation with  $15\text{ J/m}^2$  of UV but, to varying extents, resume proliferating thereafter. For our studies on 6-4PP repair, this timeline has been favourably exploited. Indeed since removal of this photoproduct is normally complete by 6–8 h post-UV, repair kinetics can be conveniently evaluated in each of G0/G1, S, and G2/M by simple gating of PI-stained populations (as we have done here and in the past [20]). However in order to monitor GG-NER of CPDs as a function of cell cycle over a 24 h period, it is necessary to further carefully control for cellular proliferation during post-UV incubations. We therefore modified our flow cytometry-based assay to include a third label, i.e., BrdU in addition to PI and anti-CPD antibody, thereby allowing positive tracking of cells which are in S phase at the time of irradiation. Fig. 2A displays a representative dot plot of BrdU staining as function of DNA content at 0 and 24 h for wild-type GM01652B

fibroblasts vs. the XPV strain XP30RO. The vertical dashed red line (delineating early- from late-S phase) and red numerals highlight the degree of cell cycling within S phase over a 24 h period. Repair analysis of the appropriate populations (i.e., gated as shown in Fig. 2A) shows that CPD removal is significantly reduced uniquely during S phase in either  $\text{pol}\eta$ -deficient XP30RO, or as previously shown in ATR-deficient F02-98 [20], whereas normal repair during all phases is observed in wild-type GM01652B (Fig. 2B). Our results displayed thus far demonstrate that cultured primary XPV-skin fibroblasts irradiated with  $15\text{ J/m}^2$  of UV are defective in genome-wide removal of both 6-4PPs and CPDs exclusively during S phase, and that this defect persists up to at least 24 h post-UV.

### 3.2. Defective SPR in XPV cells is attributable to loss of functional $\text{pol}\eta$

In order to test whether loss of functional  $\text{pol}\eta$  underlies the observed SPR defect in XPV cells, we determined cell cycle-specific kinetics of 6-4PP removal in SV40-transformed XP30ROsv vs. the same strain wherein wild-type  $\text{pol}\eta$  had been ectopically re-expressed (XP30ROsv- $\text{pol}\eta/\text{cl6}$ ) [32,33] (Fig. 3A). As expected based on our results in primary XPV cells,  $\text{pol}\eta$ -deficient XP30ROsv exhibits marked deficiency in 6-4PP repair uniquely during S phase; however, of note, this defect is significantly rescued in XP30ROsv- $\text{pol}\eta/\text{cl6}$  (Fig. 3B and C). Furthermore primary LL lung fibroblasts were transfected with siRNAs targeting  $\text{pol}\eta$ , resulting in strong knockdown of the protein (Fig. 3D). In full accord with the results for XP30ROsv vs. XP30ROsv- $\text{pol}\eta/\text{cl6}$ ,  $\text{pol}\eta$ -depleted LL cells manifest dramatic loss of SPR but normal repair during G0/G1 or G2/M, whereas DNA photoproduct removal is unaffected during all phases in counterparts expressing control scrambled siRNAs (Fig. 3E).

### 3.3. Proper-nuclear localization, -focus formation, and -PCNA binding activity of $\text{pol}\eta$ appear necessary for efficient SPR in UV-exposed skin fibroblasts

Towards elucidating the functional basis of the requirement for  $\text{pol}\eta$  in SPR, two previously characterized EGFP-tagged  $\text{pol}\eta$  domain variants were constructed: (i) EGFP- $\text{pol}\eta$ - $\Delta\text{Ct}$  (initially designated  $\text{pol}\eta$ -642n) [32], carrying a 70 amino acid C-terminal truncation which eliminates the canonical nuclear localization signal NLS2 at positions 682–698, and (ii) EGFP- $\text{pol}\eta$ -PIP1/2, mutated in the two PCNA-interacting domains (PIP1 and PIP2) normally

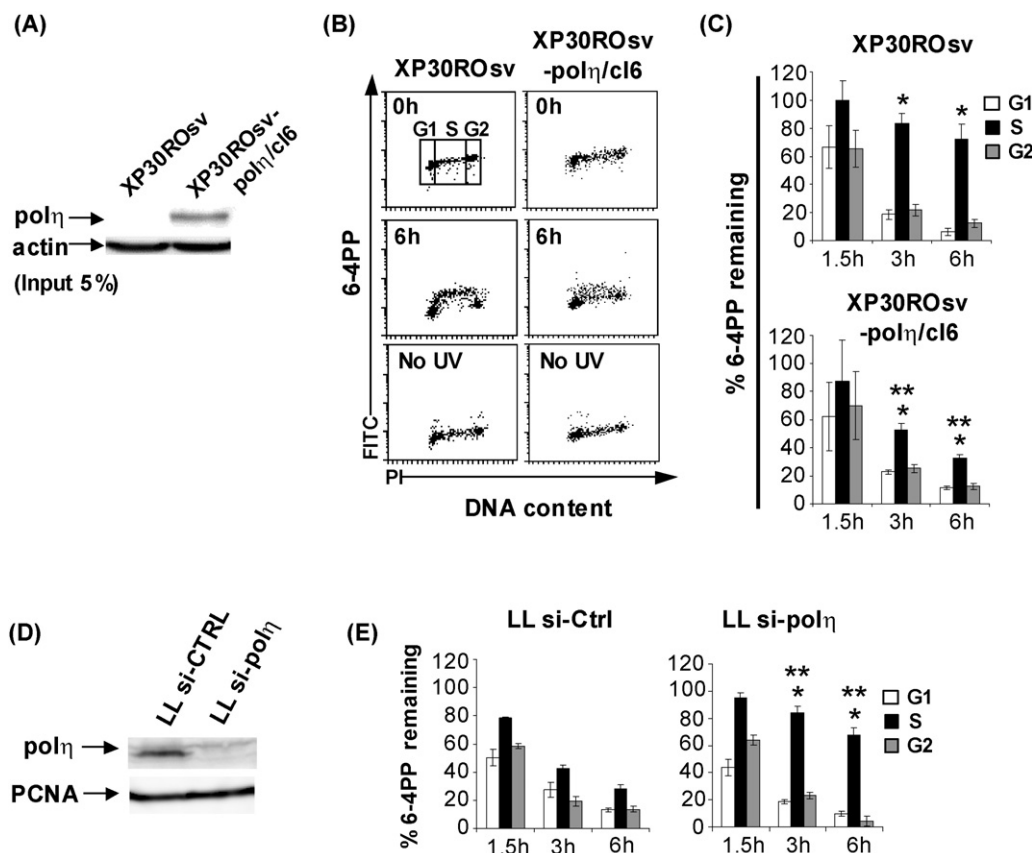


**Fig. 3.** Defective SPR in XPV cells is attributable to loss of functional  $\text{pol}\eta$ . (A) Detection of  $\text{pol}\eta$  in XP30ROsv vs. XP30ROsv- $\text{pol}\eta/\text{cl6}$  by immunoprecipitation and Western blotting. (B) Representative bivariate distributions of 6-4PP (FITC) vs. DNA content (PI) in XP30ROsv and XP30ROsv- $\text{pol}\eta/\text{cl6}$  irradiated with  $15\text{ J/m}^2$  of UV. (C) Graphical depiction of repair in XP30ROsv vs. XP30ROsv- $\text{pol}\eta/\text{cl6}$  irradiated with  $15\text{ J/m}^2$  of UV. Shown is the mean  $\pm$  SEM of three independent experiments. \* $p < 0.05$ ; two-tailed paired  $t$ -test (S phase relative to G1). \*\* $p < 0.05$ ; two-tailed unpaired  $t$ -test comparing SPR in XP30ROsv- $\text{pol}\eta/\text{cl6}$  vs. XP30ROsv. (D) Detection of  $\text{pol}\eta$  in primary LL lung fibroblasts expressing either siRNAs targeting  $\text{pol}\eta$  or control scrambled siRNAs. (E) Graphical depiction of repair in LL fibroblasts irradiated with  $15\text{ J/m}^2$  of UV. Shown is the mean  $\pm$  SEM of three independent experiments. \* $p < 0.05$ ; two-tailed paired  $t$ -test (S phase relative to G1). \*\* $p < 0.05$ ; two-tailed unpaired  $t$ -test comparing SPR in LL si- $\text{pol}\eta$  vs. LL si-CTRL.

required for accumulation at DNA replication foci, and for DNA synthetic activity, of  $\text{pol}\eta$  [34]. Each of the above mutants, in addition to wild-type  $\text{pol}\eta$  (EGFP- $\text{pol}\eta$ -wt), was stably expressed in XP30ROsv cells (Fig. 4A). In line with prior work [32], EGFP- $\text{pol}\eta$ - $\Delta\text{Ct}$  exhibits both nuclear and cytoplasmic localization, as contrasted with the primarily nuclear localization of EGFP- $\text{pol}\eta$ -wt (Fig. 4B). In addition EGFP- $\text{pol}\eta$ -PIP1/2, although proficient in nuclear localization (Fig. 4B) as previously observed [34], is defective relative to EGFP- $\text{pol}\eta$ -wt in either spontaneous- or UV-induced  $\text{pol}\eta$  nuclear focus formation (Fig. 4C). Further analysis revealed that EGFP- $\text{pol}\eta$ -wt, when ectopically expressed in XP30ROsv, restores SPR of 6-4PPs to a normal level as determined at 6 h post-UV (Fig. 4D, compare with Fig. 3C). In contrast, expression of either EGFP- $\text{pol}\eta$ - $\Delta\text{Ct}$  or EGFP- $\text{pol}\eta$ -PIP1/2 in XP30ROsv failed to engender any improvement in repair capacity. These data indicate that both proper subcellular localization, focus formation, and PCNA binding activity of  $\text{pol}\eta$  are required to ensure the efficient removal of UV-induced damage in replicating cells.

#### 3.4. Abrogation of semiconservative DNA synthesis prior to UV exposure rescues defective SPR in either XPV- or Seckel syndrome fibroblasts

ATR and  $\text{pol}\eta$  are well known to play central roles in maintaining replication fork stability in UV-exposed cells (see Section 4), and we have demonstrated herein and elsewhere [20] that both proteins are required for repair of UV-induced DNA damage uniquely during

S phase. As such it is tempting to speculate upon a link between DNA replication and GG-NER of replication-blocking DNA adducts. To approach this possibility, we evaluated 6-4PP removal as a function of cell cycle in XP30ROsv vs. XP30ROsv- $\text{pol}\eta/\text{cl6}$ , each of which had been treated or not prior to UV irradiation with either (i)  $15\text{ }\mu\text{g/ml}$  of aphidicolin, a powerful inhibitor of replicative DNA polymerases [35], or (ii)  $10\text{ mM}$  hydroxyurea (HU), which precludes semiconservative DNA synthesis via ribonucleotide reductase inhibition and subsequent depletion of dNTP pools [36]. DNA replication was profoundly reduced following treatment with either inhibitor as determined by BrdU incorporation (Fig. 5A). In accord with results shown in Fig. 3C, XP30ROsv exhibits abrogation of 6-4PP removal uniquely during S phase as determined at 6 h post-UV; however under conditions where DNA synthesis is inhibited by either aphidicolin or HU pre-treatment, SPR capacity is significantly restored (Fig. 5B). As expected, XP30ROsv- $\text{pol}\eta/\text{cl6}$  cells manifest a much more moderate SPR defect relative to XP30ROsv (compare with Fig. 3C) which, interestingly, also appears to be rescued by pre-treatment with aphidicolin. We next evaluated the effects of DNA synthesis inhibition on SPR of 6-4PP in ATR-deficient F02-98 Seckel syndrome fibroblasts, compared with the closely related wild-type strain 1BR. Incubation with aphidicolin prior to UV irradiation markedly reduced DNA synthesis in both strains (Fig. 5C). As fully anticipated based on our previous findings [20], F02-98 displayed profound deficiency in SPR as determined at 6 h post-UV; moreover, mirroring the results for XP30ROsv, aphidicolin treatment completely resolved this defect (Fig. 5D). The above data

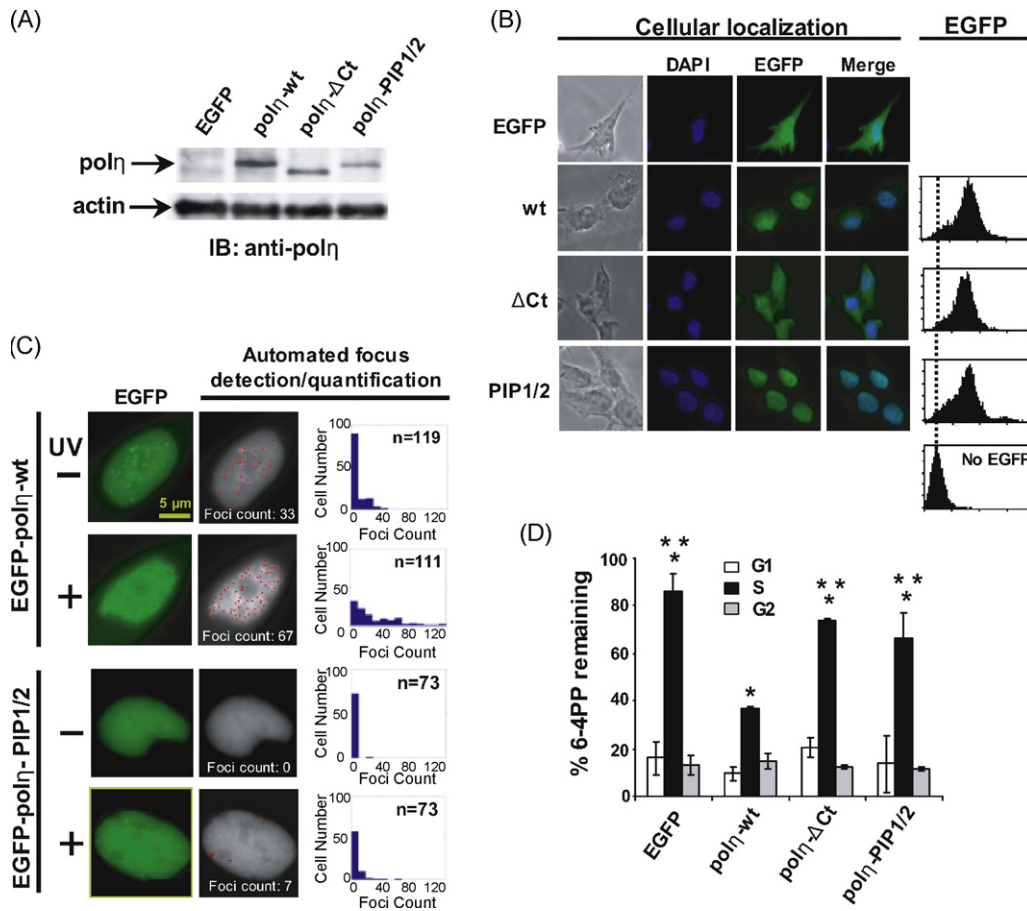


**Fig. 4.** Analysis of XP30ROsv cells ectopically expressing EGFP-tagged polη variants. (A) Stable expression of EGFP-polη variants in XP30ROsv detected by immunoprecipitation and Western blotting. (B) Left panel, cellular localization of EGFP-polη variants in XP30ROsv cells as determined by EGFP autofluorescence in fixed unirradiated cells. Right panel: EGFP autofluorescence peaks in living XP30ROsv cells. (C) Quantification of EGFP-polη foci in living XP30ROsv cells expressing either EGFP-polη-PIP1/2 or EGFP-polη-wt. In each case, the same cells were imaged before (-) and 1.5 h after (+) irradiation with 15 J/m<sup>2</sup> of UV. Shown on the left are representative nuclei and automated focus counts (see Section 2). Histograms on the right show automated determinations of focus count distribution for the indicated number of cells. (D) Graphical depiction of 6-4PP removal as determined at 6 h following exposure to 15 J/m<sup>2</sup> of UV in XP30ROsv cells expressing the indicated EGFP-polη-variants. Shown is the mean ± SEM from three independent experiments. \**p* < 0.05; two-tailed paired *t*-test (S phase relative to G1). \*\**p* < 0.05; two-tailed unpaired *t*-test comparing S phase repair in XP30ROsv cells expressing EGFP-polη-wt vs. empty vector (EGFP) or EGFP-polη domain mutants.

indicate that, under conditions where the formation of blocked replication forks at UV-damaged sites in DNA is prevented, defective SPR in both XPV- and Seckel syndrome-cells is significantly rescued.

**3.5. Defective SPR is not observed in XPV or Seckel syndrome fibroblasts irradiated with a relatively low dose (5 J/m<sup>2</sup>) of UV**

The above experiments were all performed on cells treated with 15 J/m<sup>2</sup> of 254-nm UV. Doses within this range (i.e., 10–20 J/m<sup>2</sup>) have been extensively employed over the years to evaluate GG-NER kinetics in cultured human cells. However it should be emphasized that in general CPD repair rates can vary significantly with dose, although the underlying reasons are not entirely clear [37]. In light of this, our triple-labeling approach was used to investigate the extent to which defective SPR, as observed in XPV- and Seckel syndrome-cells irradiated with 15 J/m<sup>2</sup> of UV, might also occur at a lower dose of 5 J/m<sup>2</sup>. A representative dot plot of BrdU staining as a function of DNA content at 0 and 24 h for wild-type GM01652B fibroblasts vs. the XPV strain XP30RO irradiated with 5 J/m<sup>2</sup> of UV is shown (Fig. 6A). It is apparent that GM01652B resumes proliferating very rapidly at the lower dose such that it is not possible under our assay conditions to accurately measure CPD repair at any point after 12 h post-UV, or even to differentiate between G0/G1

and G2/M cells. Indeed the gated populations in Fig. 6A, designated “G1/G2”, actually represent a mixture of cells which were in either G0/G1 or G2/M at the time of irradiation. On the other hand in the case of both XPV- and Seckel syndrome fibroblasts recovery of DNA synthesis post-UV is, as expected, considerably slower than wild-type fibroblasts, rendering it possible to compare repair kinetics in the former two strains up to 24 h post-UV during S vs. “G1/G2”. Relative to the situation for cells irradiated with 15 J/m<sup>2</sup> of UV (Fig. 2), following exposure to 5 J/m<sup>2</sup> both XP30RO and F02-98 each exhibit rates of CPD repair during S that are more comparable to those during G1/G2 (Fig. 6B). The overall data suggest the existence of a dose threshold for SPR inhibition in the case of either polη- or ATR-deficient cells. Furthermore it is possible that this threshold may be determined by levels of replication stress, as such levels are expected to be considerably lower in cells irradiated with 5 J/m<sup>2</sup> vs. 15 J/m<sup>2</sup> of UV.

**4. Discussion**

Here we demonstrate that patient-derived XPV-skin fibroblasts irradiated with 15 J/m<sup>2</sup> of 254-nm UV are characterized by a significant reduction in GG-NER efficiency uniquely during S phase due to loss of functional polη. Further evidence is presented suggesting that this repair defect is rescued in either XPV- or Seckel

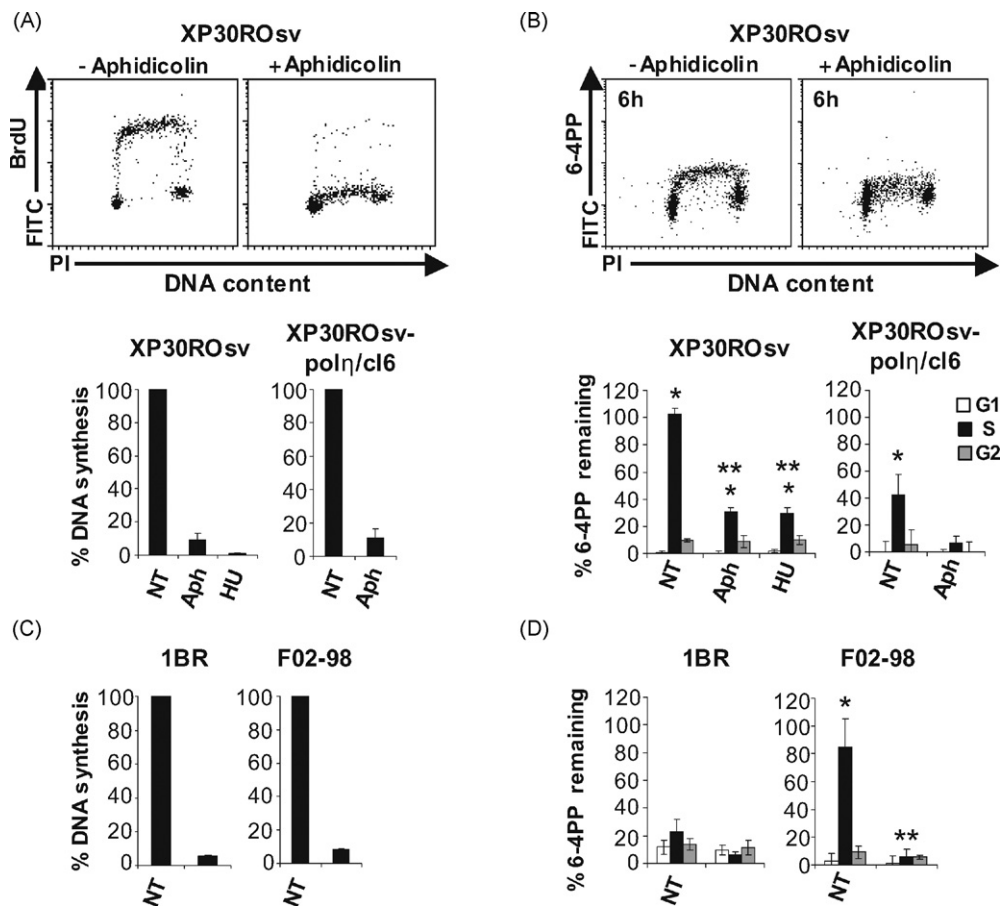


**Fig. 5.** Defective SPR in XPV fibroblasts is rescued by treatment with DNA synthesis inhibitors prior to UV exposure. (A) Upper panel: representative dot plot showing BrdU incorporation in XP30ROsv cells pre-treated or not with aphidicolin. Lower panel: graphical depiction of percent DNA synthesis inhibition in XP30ROsv and XP30ROsv-polη/cl6 pre-treated or not with HU and/or aphidicolin. (B) Upper panel: representative dot plot showing 6-4PP repair as function of DNA content at 6h post-UV (15J/m<sup>2</sup>) in XP30ROsv vs. XP30ROsv-polη/cl6 cells pre-treated or not with aphidicolin. Lower panel: graphical depiction of 6-4PP repair as a function of cell cycle at 6h post-UV in XP30ROsv vs. XP30ROsv-polη/cl6 pre-treated or not with aphidicolin or HU. (C) Graphical depiction of percent DNA synthesis inhibition in 1BR wild-type and F02-98 Seckel syndrome skin fibroblasts pre-treated or not with aphidicolin. (D) Graphical depiction of 6-4PP repair at 6h post-UV as a function of cell cycle in 1BR vs F02-98 pre-treated or not with aphidicolin. Shown is the mean ± SEM of three independent experiments \**p* < 0.05; two-tailed paired *t*-test (S phase relative to G1). \*\**p* < 0.05; two-tailed unpaired *t*-test comparing S phase repair in aphidicolin or HU treated vs. untreated (NT) cells.

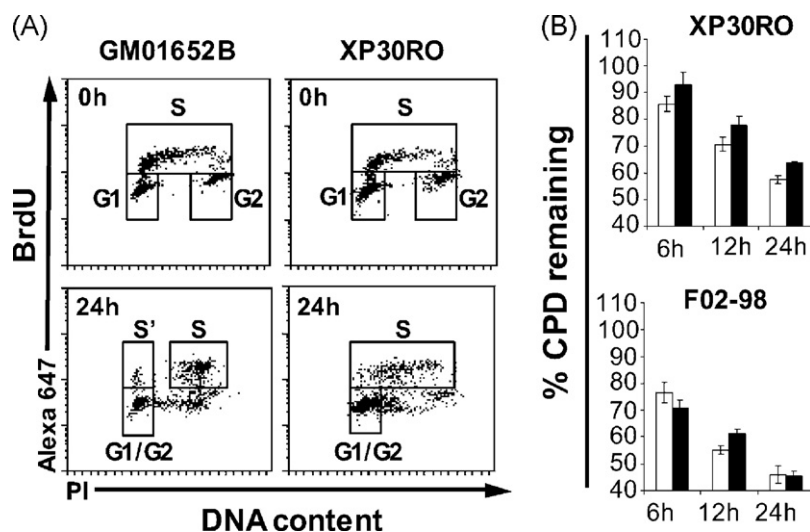


**Fig. 6.** Normal SPR of CPDs in XPV- and Seckel syndrome-cells irradiated with 5J/m<sup>2</sup> of UV. (A) Bivariate distribution of BrdU incorporation (Alexa 647) vs. DNA content (PI) in GM01652B vs. XP30RO at 0h vs. 24h following irradiation with 5J/m<sup>2</sup> of UV. (B) Graphical depictions of cell cycle-specific CPD repair in XP30RO and F02-98 cells treated with 5J/m<sup>2</sup> of UV. G1/G2 denotes a mixture of cells that were in either G0/G1 or G2/M at the time of irradiation (see Section 3). Indeed, at 5J/m<sup>2</sup> of UV, G2/M cells divide relatively rapidly and mix with cells initially in G1, and therefore cannot be analyzed separately. For GM01652B, at 5J/m<sup>2</sup>, repair cannot be monitored at 24h post-UV since a proportion of cells in S phase at the time of irradiation (S') have traversed G2 and undergone division. Shown is the mean ± SEM of three independent experiments.



syndrome-cells if the formation of blocked replication forks post-UV is either prevented or substantially reduced, i.e., following, respectively, pharmacological inhibition of DNA synthesis prior to UV irradiation, or exposure to a relatively low UV dose ( $5\text{ J/m}^2$ ). Although wavelengths within the UV-C region (190–280 nm) are vastly attenuated at the surface of the earth by stratospheric ozone, we note that  $15\text{ J/m}^2$  of 254-nm UV has been shown to generate a yield of DNA photoproducts comparable to that induced following 1–2 h irradiation with natural sunlight [38,39]. As such it is possible that our results in cultured cells could harbour implications for XPV pathogenesis. As emphasized earlier, the extreme UV-hypermutable leading to skin cancer development in XPV patients is clearly attributable to defective TLS. Specifically, in the absence of  $\text{pol}\eta$ , XPV cells are able to recruit the activities of  $\text{pol}\kappa$  and  $\text{pol}\iota$  which (in cooperation with the B-family DNA polymerase  $\zeta$ ) can efficiently bypass CPDs thereby promoting cell survival; however in doing so these “backup” polymerases, each being orders of magnitude more error-prone than  $\text{pol}\eta$  when replicating UV-damaged templates, generate excessive errors of nucleotide incorporation [19]. Therefore in instances where XPV patients would sustain high enough doses of natural sunlight (i.e., which induce levels of DNA damage equivalent to or greater than  $15\text{ J/m}^2$  of 254-nm UV), we speculate that defective SPR of highly promutagenic CPDs may to some extent promote XPV-associated hypermutability by acting synergistically with  $\text{pol}\kappa/\iota$ -mediated highly error-prone TLS past these photoproducts. We further speculate, again in response to high enough doses of natural sunlight, that the incapacity to remove replication-blocking CPDs and 6-4PPs during S phase might partially contribute to the characteristic DNA synthesis defect in XPV. This contribution would be in addition to the primary one provided by deficient  $\text{pol}\eta$ -mediated CPD bypass; indeed delayed replication restart has been observed in XPV cells irradiated with doses as low as  $2\text{ J/m}^2$  [40], where defective SPR is not expected to occur.

It should be noted that two previous studies (mentioned in the Introduction) used a sensitive radioimmunoassay to probe the possibility that GG-NER of 6-4PPs might be regulated as a function of cell cycle in XPV strains. Firstly EBV-transformed XPV B-lymphocytes (strain XPPHBE), synchronized by centrifugal elutriation and treated with  $12\text{ J/m}^2$  of UV, displayed no differences in repair efficiency during S phase relative to G0/G1 or G2/M [9]. The divergence here with our results may partially reflect the purity of the S phase populations analyzed, i.e., 60% in the aforementioned study compared with essentially 100% in our case. Furthermore whereas it was later shown that XPPHBE bears a frameshift mutation in one *POLH* allele, no sequence alterations were detected in the other allele which was also found to be expressed at only 20% the level of the mutated counterpart [41]. Thus XPPHBE may express some wild-type  $\text{pol}\eta$  which could significantly enhance SPR. Secondly, another major investigation on XPV-skin fibroblasts irradiated with  $6\text{ J/m}^2$  of UV also failed to observe any cell cycle-specific differences in GG-NER efficiency [13]. This discrepancy may be readily reconciled by our finding here that defective SPR in XPV cells is clearly observed at  $15\text{ J/m}^2$  of UV, but is considerably less pronounced at lower doses in the range of  $5\text{ J/m}^2$ .

It is becoming increasingly apparent that various Y-family polymerases can mediate cellular processes other than TLS [42,43]. Of particular interest here it was unexpectedly shown that  $\text{pol}\kappa$ -null murine embryonic fibroblasts are defective in the DNA repair synthesis step of NER (although not in an S phase-specific manner) [44]. While a similar role for  $\text{pol}\eta$  in DNA repair synthesis during S phase cannot be categorically ruled out, we are nonetheless confident that loss of SPR capacity in XPV fibroblasts is attributable to a defect in some step of GG-NER which precedes gapfilling (i.e., in lesion recognition or -incision/excision). Indeed our flow

cytometry-based repair assay specifically measures the complete removal (excision) of UV DNA photoproducts, and would not competently reveal defects in DNA repair synthesis *per se*, i.e., assuming that this latter step is carried out largely or entirely post-excision as has been proposed [45–47].

How then might loss of functional  $\text{pol}\eta$  engender virtually complete loss of SPR, while exerting no effect on repair during G0/G1 or G2/M? We recently reported that ATR-deficient Seckel syndrome fibroblasts, like XPV fibroblasts, exhibit a significant S phase-specific GG-NER defect [20]. Following UV exposure, ATR rapidly phosphorylates a multitude of substrates that together stabilize stalled replication forks and facilitate DNA synthesis restart [48]. As such deficiency in ATR signaling causes abnormal persistence and eventual collapse of blocked replication forks, leading to induction of highly genotoxic DSBs at sites of UV-damage [49]. Moreover enhanced H2AX phosphorylation has been noted in XPV vs. normal cells post-UV, indicating that the former also suffer a relative increase in DSB formation at collapsed replication forks [50,51]. Finally our results in either XPV- or Seckel syndrome-cells treated with DNA synthesis inhibitors or low dose UV suggest that defective SPR can be fully rescued by precluding, or substantially reducing below some threshold, the formation of blocked replication forks at UV-adducted sites in DNA.

Considering the above commonalities between XPV- and Seckel syndrome-cells we speculate that, in general, attenuation of GG-NER may actually serve to promote cellular survival specifically in S phase populations undergoing excessive replication stress. We emphasize that such a mechanism may not depend upon any direct enzymatic role in GG-NER for either ATR or  $\text{pol}\eta$ , but rather solely upon the ability of these proteins to mitigate replication stress which in turn positively influences repair. Precisely how this occurs remains to be established. It should be noted that higher levels of replication stress engender corresponding increases in large tracts of single-strand DNA due to functional uncoupling of DNA synthetic enzymes at stalled replication forks; furthermore replication protein-A (RP-A) avidly binds to such tracts, an event that is required for activation of ATR signaling [52]. It is therefore conceivable and consistent with our data that, once levels of replication stress reach a particular threshold, RP-A becomes effectively sequestered. This may abrogate removal of UV-induced DNA damage in the genome overall (exclusively in replicating cells), as sufficient levels of free RP-A are required to carry out the pre-incision and gapfilling steps of GG-NER [53]. This hypothetical model has received some experimental support in the case of yeast during meiosis, where the existence of excess single-stranded DNA appears to reduce the efficiency of double-strand-break repair through RP-A sequestration [54]. Further support is provided by the very recent demonstration that XPV cells are subject to elevated levels of fork stalling that correlates with the generation of extensive ssDNA regions (which are ostensibly bound by RP-A) [55]. Finally we note that in addition to the above passive mechanism based on RP-A sequestration, considering the status of stalled replication forks *per se* as powerful signals for initiating various mechanisms of self-stabilization, we speculate that genome-wide inhibition of GG-NER during S phase might somehow be actively regulated.

Whatever the precise mechanistic underpinnings, a significant reduction in “unwanted” NER-mediated DNA incisions under conditions of excessive replication stress may actually serve to promote cellular survival by forestalling the “conversion” of numerous CPDs and 6-4PPs located at persistently stalled replication forks into considerably more lethal DSBs [56]. In the case of XPV cells, such a reduction of DSB formation may be needed to facilitate alternative pathways, e.g., error-free template switching [57], and/or error-prone bypass using backup TLS polymerases [19], designed to resolve blocked replication forks and stimulate the resumption

of DNA synthesis as rapidly as possible. However, while ablation of SPR in XPV patients might be considered potentially “beneficial” at the cellular level by increasing survival, the accompanying effect at the organismal level, i.e., remarkably elevated levels of sunlight-induced mutation and cancer, is of course disastrous.

### Conflict of interest statement

The authors declare that there are no conflicts of interest.

### Acknowledgements

This work was supported by an operating grant awarded to E.A.D. from the Canadian Institutes of Health Research (CIHR) and to S.C. by the Natural Sciences and Engineering Research Council of Canada (NSERC). J.M.B. is supported by an NSERC doctoral research award. The authors are grateful to Drs. El Bachir Affar, Dindial Ramotar, and James Daley for critical reading of the manuscript.

### References

- [1] E.C. Friedberg, G.C. Walker, W. Siede, R.D. Wood, R.A. Schultz, T. Ellenberger (Eds.), *DNA Repair and Mutagenesis*, 2nd ed., ASM Press, Washington, DC, 2006.
- [2] L.C. Gillet, O.D. Scharer, Molecular mechanisms of mammalian global genome nucleotide excision repair, *Chem. Rev.* 106 (2006) 253–276.
- [3] P.C. Hanawalt, G. Spivak, Transcription-coupled DNA repair: two decades of progress and surprises, *Nat. Rev. Mol. Cell Biol.* 9 (2008) 958–970.
- [4] J.E. Cleaver, Defective repair replication of DNA in xeroderma pigmentosum, *Nature* 218 (1968) 652–656.
- [5] K.H. Kraemer, M.M. Lee, J. Scotto, DNA repair protects against cutaneous and internal neoplasia: evidence from xeroderma pigmentosum, *Carcinogenesis* 5 (1984) 511–514.
- [6] J.E. Cleaver, Xeroderma pigmentosum: variants with normal DNA repair and normal sensitivity to ultraviolet light, *J. Invest. Dermatol.* 58 (1972) 124–128.
- [7] J.H. Robbins, W.R. Levis, A.E. Miller, Xeroderma pigmentosum epidermal cells with normal UV-induced thymidine incorporation, *J. Invest. Dermatol.* 59 (1972) 402–408.
- [8] W.J. Kleijer, E.A. de Weerd-Kastelein, M.L. Sluyter, W. Keijzer, J. de Wit, D. Bootsma, UV-induced DNA repair synthesis in cells of patients with different forms of xeroderma pigmentosum and of heterozygotes, *Mutat. Res.* 20 (1973) 417–428.
- [9] D.L. Mitchell, J.E. Cleaver, M.P. Lowery, R.R. Hewitt, Induction and repair of (6-4) photoproducts in normal human and xeroderma pigmentosum variant cells during the cell cycle, *Mutat. Res.* 337 (1995) 161–167.
- [10] T. Hiramoto, T. Matsunaga, M. Ichihashi, O. Nikaido, Y. Fujiwara, Y. Mishima, Repair of 254 nm ultraviolet-induced (6-4) photoproducts: monoclonal antibody recognition and differential defects in xeroderma pigmentosum complementation groups A, D, and variant, *J. Invest. Dermatol.* 93 (1989) 703–706.
- [11] D.L. Mitchell, C.A. Haipek, J.M. Clarkson, Xeroderma pigmentosum variant cells are not defective in the repair of (6-4) photoproducts, *Int. J. Radiat. Biol.* 52 (1987) 201–205.
- [12] A. Hessel, R.J. Siegle, D.L. Mitchell, J.E. Cleaver, Xeroderma pigmentosum variant with multisystem involvement, *Arch. Dermatol.* 128 (1992) 1233–1237.
- [13] Y.C. Wang, V.M. Maher, D.L. Mitchell, J.J. McCormick, Evidence from mutation spectra that the UV hypermutability of xeroderma pigmentosum variant cells reflects abnormal, error-prone replication on a template containing photoproducts, *Mol. Cell Biol.* 13 (1993) 4276–4283.
- [14] V.M. Maher, L.M. Ouellette, R.D. Curren, J.J. McCormick, Frequency of ultraviolet light-induced mutations is higher in xeroderma pigmentosum variant cells than in normal human cells, *Nature* 261 (1976) 593–595.
- [15] A.R. Lehmann, S. Kirk-Bell, C.F. Arlett, M.C. Paterson, P.H. Lohman, E.A. de Weerd-Kastelein, D. Bootsma, Xeroderma pigmentosum cells with normal levels of excision repair have a defect in DNA synthesis after UV-irradiation, *Proc. Natl. Acad. Sci. U.S.A.* 72 (1975) 219–223.
- [16] C. Masutani, R. Kusumoto, A. Yamada, N. Dohmae, M. Yokoi, M. Yuasa, M. Araki, S. Iwai, K. Takio, F. Hanaoka, The XPV (xeroderma pigmentosum variant) gene encodes human DNA polymerase  $\eta$ , *Nature* 399 (1999) 700–704.
- [17] S.D. McCulloch, T.A. Kunkel, The fidelity of DNA synthesis by eukaryotic replicative and translesion synthesis polymerases, *Cell Res.* 18 (2008) 148–161.
- [18] S.L. Yu, R.E. Johnson, S. Prakash, L. Prakash, Requirement of DNA polymerase  $\eta$  for error-free bypass of UV-induced CC and TC photoproducts, *Mol. Cell Biol.* 21 (2001) 185–188.
- [19] O. Ziv, N. Geacintov, S. Nakajima, A. Yasui, Z. Livneh, DNA polymerase  $\zeta$  cooperates with polymerases  $\kappa$  and  $\iota$  in translesion DNA synthesis across pyrimidine photodimers in cells from XPV patients, *Proc. Natl. Acad. Sci. U.S.A.* 106 (2009) 11552–11557.
- [20] Y. Auclair, R. Rouget, E.B. Affar, E.A. Drobetsky, ATR kinase is required for global genomic nucleotide excision repair exclusively during S phase in human cells, *Proc. Natl. Acad. Sci. U.S.A.* 105 (2008) 17896–17901.
- [21] R. Rouget, Y. Auclair, M. Loignon, E.B. Affar, E.A. Drobetsky, A sensitive flow cytometry-based nucleotide excision repair assay unexpectedly reveals that mitogen-activated protein kinase signalling does not regulate the removal of UV-induced DNA damage in human cells, *J. Biol. Chem.* 283 (2007) 5533–5541.
- [22] R.R. Laposla, L. Feeney, J.E. Cleaver, Recapitulation of the cellular xeroderma pigmentosum-variant phenotypes using short interfering RNA for DNA polymerase  $\eta$ , *Cancer Res.* 63 (2003) 3909–3912.
- [23] M. Thakur, M. Wernick, C. Collins, C.L. Limoli, E. Crowley, J.E. Cleaver, DNA polymerase  $\eta$  undergoes alternative splicing, protects against UV sensitivity and apoptosis, and suppresses Mre11-dependent recombination, *Genes Chromosomes Cancer* 32 (2001) 222–235.
- [24] N. Otsu, A threshold selection method from gray-level histograms, *IEEE Trans. Syst. Man Cybern.* 9 (1979) 62–66.
- [25] C.F. Arlett, S.A. Harcourt, B.C. Broughton, The influence of caffeine on cell survival in excision-proficient and excision-deficient xeroderma pigmentosum and normal human cell strains following ultraviolet-light irradiation, *Mutat. Res.* 33 (1975) 341–346.
- [26] D.L. Mitchell, C.A. Haipek, J.M. Clarkson, (6-4) Photoproducts are removed from the DNA of UV-irradiated mammalian cells more efficiently than cyclobutane pyrimidine dimers, *Mutat. Res.* 143 (1985) 109–112.
- [27] V.O. Melnikova, H.N. Ananthaswamy, Cellular and molecular events leading to the development of skin cancer, *Mutat. Res.* 571 (2005) 91–106.
- [28] S. Adimoolam, C.X. Lin, J.M. Ford, The p53-regulated cyclin-dependent kinase inhibitor, p21 (cip1, waf1, sdi1), is not required for global genomic and transcription-coupled nucleotide excision repair of UV-induced DNA photoproducts, *J. Biol. Chem.* 276 (2001) 25813–25822.
- [29] J. Tang, G. Chu, Xeroderma pigmentosum complementation group E and UV-damaged DNA-binding protein, *DNA Repair* 1 (2002) 601–616.
- [30] A.R. Lehmann, S. Kirk-Bell, C.F. Arlett, S.A. Harcourt, E.A. de Weerd-Kastelein, W. Keijzer, P. Hall-Smith, Repair of ultraviolet light damage in a variety of human fibroblast cell strains, *Cancer Res.* 37 (1977) 904–910.
- [31] R.B. Painter, Inhibition and recovery of DNA synthesis in human cells after exposure to ultraviolet light, *Mutat. Res.* 145 (1985) 63–69.
- [32] P. Kannouche, B.C. Broughton, M. Volker, F. Hanaoka, L.H. Mullenders, A.R. Lehmann, Domain structure, localization, and function of DNA polymerase  $\eta$ , defective in xeroderma pigmentosum variant cells, *Genes Dev.* 15 (2001) 158–172.
- [33] A. Stary, P. Kannouche, A.R. Lehmann, A. Sarasin, Role of DNA polymerase  $\eta$  in the UV mutation spectrum in human cells, *J. Biol. Chem.* 278 (2003) 18767–18775.
- [34] N. Acharya, J.H. Yoon, H. Gali, I. Unk, L. Haracska, R.E. Johnson, J. Hurwitz, L. Prakash, S. Prakash, Roles of PCNA-binding and ubiquitin-binding domains in human DNA polymerase  $\eta$  in translesion DNA synthesis, *Proc. Natl. Acad. Sci. U.S.A.* 105 (2008) 17724–17729.
- [35] G. Pedrali-Noy, S. Spadari, A. Miller-Faures, A.O. Miller, J. Kruppa, G. Koch, Synchronization of HeLa cell cultures by inhibition of DNA polymerase  $\alpha$  with aphidicolin, *Nucleic Acids Res.* 8 (1980) 377–387.
- [36] J.A. Wright, A.K. Chan, B.K. Choy, R.A. Hurta, G.A. McClarty, A.Y. Tagger, Regulation and drug resistance mechanisms of mammalian ribonucleotide reductase, and the significance to DNA synthesis, *Biochem. Cell Biol.* 68 (1990) 1364–1371.
- [37] R. Greinert, O. Boguhn, D. Harder, E.W. Breitbart, D.L. Mitchell, B. Volkmer, The dose dependence of cyclobutane dimer induction and repair in UVB-irradiated human keratinocytes, *Photochem. Photobiol.* 72 (2000) 701–708.
- [38] Z. Kuluncsics, D. Perdiz, E. Brulay, B. Muel, E. Sage, Wavelength dependence of ultraviolet-induced DNA damage distribution: involvement of direct or indirect mechanisms and possible artefacts, *J. Photochem. Photobiol.* 49 (1999) 71–80.
- [39] J.H. Yoon, C.S. Lee, T.R. O'Connor, A. Yasui, G.P. Pfeifer, The DNA damage spectrum produced by simulated sunlight, *J. Mol. Biol.* 299 (2000) 681–693.
- [40] S.K. Bullock, W.K. Kaufmann, M. Cordeiro-Stone, Enhanced S phase delay and inhibition of replication of an undamaged shuttle vector in UVC-irradiated xeroderma pigmentosum variant, *Carcinogenesis* 22 (2001) 233–241.
- [41] R.E. Johnson, C.M. Kondratik, S. Prakash, L. Prakash, hRAD30 mutations in the variant form of xeroderma pigmentosum, *Science* 285 (1999) 263–265.
- [42] A.R. Lehmann, New functions for Y family polymerases, *Mol. Cell* 24 (2006) 493–495.
- [43] L. Rey, J.M. Sidorova, N. Puget, F. Boudsocq, D.S. Biard, R.J. Monnat Jr., C. Cazaux, J.S. Hoffmann, Human DNA polymerase  $\eta$  is required for common fragile site stability during unperturbed DNA replication, *Mol. Cell Biol.* (2009).
- [44] T. Ogi, A.R. Lehmann, The Y-family DNA polymerase  $\kappa$  (pol  $\kappa$ ) functions in mammalian nucleotide-excision repair, *Nat. Cell Biol.* 8 (2006) 640–642.
- [45] D. Mu, M. Wakasugi, D.S. Hsu, A. Sanchar, Characterization of reaction intermediates of human excision repair nuclease, *J. Biol. Chem.* 272 (1997) 28971–28979.
- [46] J.G. Moggs, K.J. Yarema, J.M. Essigmann, R.D. Wood, Analysis of incision sites produced by human cell extracts and purified proteins during nucleotide excision repair of a 1,3-intrastrand d(GpTpG)-cisplatin adduct, *J. Biol. Chem.* 271 (1996) 7177–7186.
- [47] L. Staresincic, A.F. Fagbemi, J.H. Enzlin, A.M. Gourdin, N. Wijgers, I. Dunand-Sauthier, G. Giglia-Mari, S.G. Clarkson, W. Vermeulen, O.D. Scharer, Coordination of dual incision and repair synthesis in human nucleotide excision repair, *EMBO J.* 28 (2009) 1111–1120.
- [48] K.A. Cimprich, D. Cortez, ATR: an essential regulator of genome integrity, *Nat. Rev. Mol. Cell Biol.* 9 (2008) 616–627.
- [49] A.M. Friedel, B.L. Pike, S.M. Gasser, ATR/Mec1: coordinating fork stability and repair, *Curr. Opin. Cell Biol.* 21 (2009) 237–244.

- [50] C.L. Limoli, E. Giedzinski, W.F. Morgan, J.E. Cleaver, Polymerase eta deficiency in the xeroderma pigmentosum variant uncovers an overlap between the S phase checkpoint and double-strand break repair, *Proc. Natl. Acad. Sci. U.S.A.* 99 (2000) 233–238.
- [51] C.L. Limoli, E. Giedzinski, W.M. Bonner, J.E. Cleaver, UV-induced replication arrest in the xeroderma pigmentosum variant leads to DNA double-strand breaks, gamma-H2AX formation, and Mre11 relocalization, *Proc Natl. Acad. Sci. U.S.A.* 99 (2002) 233–238.
- [52] R.D. Paulsen, K.A. Cimprich, The ATR pathway: fine-tuning the fork, *DNA Repair* 6 (2007) 953–966.
- [53] Z. He, L.A. Henriksen, M.S. Wold, C.J. Ingles, RPA involvement in the damage-recognition and incision steps of nucleotide excision repair, *Nature* 374 (1995) 566–569.
- [54] R. Johnson, V. Borde, M.J. Neale, A. Bishop-Bailey, M. North, S. Harris, A. Nicolas, A.S. Goldman, Excess single-stranded DNA inhibits meiotic double-strand break repair, *PLoS Genet.* 3 (2007) e223.
- [55] E. Despras, F. Daboussi, O. Hyrien, K. Marheineke, P.L. Kannouche, ATR/Chk1 pathway is essential for resumption of DNA synthesis and cell survival in UV-irradiated XP variant cells, *Hum. Mol. Genet.* 19 (2010) 1690–1701.
- [56] G.A. Garinis, J.R. Mitchell, M.J. Moorhouse, K. Hanada, H. de Waard, D. Van-deputte, J. Jans, K. Brand, M. Smid, P.J. van der Spek, J.H. Hoeijmakers, R. Kanaar, G.T. van der Horst, Transcriptome analysis reveals cyclobutane pyrimidine dimers as a major source of UV-induced DNA breaks, *EMBO J.* 24 (2005) 3952–3962.
- [57] D. Branzei, M. Foiani, Template switching: from replication fork repair to genome rearrangements, *Cell* 131 (2007) 1228–1230.